Contribution from the Istituto per lo Studio della Stereochimica ed Energetica dei Composti di Coordinazione, CNR, 50132 Florence, Italy

Structural Comparison of Cobalt and Nickel Complexes with CS_2 and SCNPh Molecules Stabilized by Tripodal Polyphosphine Ligands. Implications for the Nature of the Chemical Bonding in Compounds Containing C-S Linkages η^2 Coordinated to L_3M Fragments

C. BIANCHINI, D. MASI, C. MEALLI,* and A. MELI

Received October 25, 1983

The crystal structures of the complexes (triphos)Co(η^2-CS_2) (**1**), (triphos)Ni(η^2-CS_2) (**2**), (triphos)Ni(η^2-SCNPh)·0.5CH_2Cl_2 (**3**), and (np_3)Co(η^2-SCNPh)·1.33C_4H_9OH (**4**) [triphos = 1,1,1-tris((diphenylphosphino)methyl)ethane; np_3 = tris(2-(diphenylphosphino)ethyl)amine] are compared with the aim of elucidating some of the factors that influence the η^2 bonding between L_3M fragments and heteroallenes. The different population at the metal atom (d^9 or d^{10}), the substitution of a sulfur atom of CS_2 for a more electronegative grouping, and the different pyramidalization at the L_3M fragment (the rigid triphos vs. the more flexible np_3 ligand) are critically evaluated with the help of extended Hückel calculations. The calculations suggest that the HOMO in these molecules is a metal-centered $\pi_\perp$ orbital, and this agrees well with the observation that the structures of **1** and **2** are almost superimposable. However, there is also an indication that the Co-S may be stronger than the Ni-S linkage because partial π bonding is operative in the former case. A more electronegative group in the heteroallene varies somewhat the composition of the HOMO, which acquires more M-S $\pi_\perp$* antibonding character with a consequent weakening of the M-S linkage as observed in **3**. This repulsive interaction also is accompanied by some unusual geometrical distortion such as the loss of C_{3v} symmetry of the P_3M fragment formed by the rigid ligand triphos. Finally, the flexible np_3 ligand, by allowing the opening of the P-M-P angles, energetically stabilizes the adducts at the expense of the strength of the M-(η^2-CS) linkage. The information gathered from this experimental and theoretical study provides keys for the interpretation of the chemistry of complexed heteroallenes. Crystal data for the newly determined structures: $C_{42}H_{39}NiP_3S_2$ (**2**), mol wt 759.54, space group orthorhombic $Pn2_1a$, $Z = 4$, $a = 20.924$ (9) Å, $b = 17.112$ (8) Å, $c = 10.283$ (5) Å, $R = 0.048$ for 2104 observed reflections; $C_{48.5}H_{45}ClNNiP_3S$ (**3**), mol wt 861.05, space group orthorhombic $Pbac$, $Z = 8$, $a = 23.142$ (7) Å, $b = 21.429$ (7) Å, $c = 17.204$ (6) Å, $R = 0.072$ for 1499 observed reflections; $C_{54.33}H_{60.33}CoNO_{1.33}P_3S$ (**4**), mol wt 932.44, space group monoclinic $P2_1/a$, $Z = 4$, $a = 36.435$ (11) Å, $b = 10.801$ (7) Å, $c = 13.026$ (8) Å, $\beta = 97.62$ (9)°, $R = 0.074$ for 2123 observed reflections.

Introduction

The coordination chemistry of carbon disulfide is interesting even in view of the implications for the desired activation of the isoelectronic carbon dioxide by transition metals. The carbon atom of the latter triatomic is in a highly oxidized state, and even a partial reduction such as that operated by a basic metal atom upon coordination is rarely observed.[1] The relatively large abundance of CS_2 complexes indicates that the different electronegativities of the therminal atoms play an important role for the stabilization of the adducts. The substitution of a single sulfur atom with a more electronegative atom or group (O or NPh) is interesting for determining how far we can go in modeling the behavior of carbon dioxide toward coordination.

Tripodal ligands such as 1,1,1-tris((diphenylphosphino)-methyl)ethane, triphos, or tris(2-(diphenylphosphino)ethyl)-amine, np_3, have been found apt to stabilize transition-metal fragments rich of electrons such as those of cobalt or nickel in low oxidation states;[2] these fragments can be used to probe the reactivity of the various heteroallene molecules. In spite of the synthetic efforts, no simple CO_2 or COS adducts have been yet isolated; conversely, we have obtained a number of CS_2 or SCNPh complexes including some unprecedented nickel(0) mononuclear species.[3] Here, we report a comparative structural study of the following complexes: (triphos)-Co(η^2-CS_2)[3a] (**1**), (triphos)Ni(η^2-CS_2)[3b] (**2**), (triphos)Ni-(η^2-SCNPh)·0.5CH_2Cl_2[3c] (**3**), and (np_3)Co(η^2-SCNPh)·1.33C_4H_9OH[3d] (**4**). The structure of **1** has been previously described in some detail,[3a] and a preliminary account of the structure of **3** has appeared.[3c] The above series of structures allows an evaluation of some important effects on the molecular geometries. One of them is just related to the replacement of the uncoordinated sulfur atom of CS_2 with the NPh grouping. One can also compare the effects of substitution of the cobalt with the nickel atom (hence a variation of total electron counts) within an unchanged ligand framework; finally, the influence of the terminal coligands is investigated by replacing the rigid triphos with the more flexible np_3 ligand.

All of these points are checked against the findings and the extensions of a recent extended Hückel MO investigation[4] for this type of adduct in the attempt of gaining deeper insight of the bonding capabilities of CX_2 triatomics toward transition-metal fragments. The reader must be warned that the analysis is generally complicated by the low or null symmetry of the complexes. Only clear-cut effects are emphasized throughout the paper.

Experimental Section

Collection and Reduction of X-ray Intensity Data. By using a Philips PW 1100 automated diffractometer with Mo Kα radiation monochromatized with a graphite crystal, we determined the orientation matrices and the lattice parameters of the crystalline samples of each compound. The number of orienting reflections varied between 18 and 25 whereas their θ range was restricted between 7 and 12°. Crystal data and various experimental variables used during the process of lattice determination and data collection are given in Table I. The observed intensities were corrected for Lorentz and polarization effects and normalized by applying factors obtained by interpolation between measurements of three standard reflections (monitored every 2 h). A correction for the absorption effect was made by using measurements of the crystal bonding planes to calculate transmission factors. These ranged between 0.93 and 0.86, 0.92 and 0.86, and 0.93 and 0.89 for **2**-**4**, respectively.

(1) For a comprehensive description and reference list of reactions of CO_2 with transition-metal complexes see: Sneeden, R. P. A. "Comprehensive Organometallic Chemistry"; Wilkinson, G., Stone, F. G. A., Abel, E. W., Eds.; Pergamon Press: New York, 1982; Vol. 8, p 225.
(2) Sacconi, L.; Mani, F. *Transition Met. Chem. (N.Y.)* **1982**, *8*, 179.
(3) (a) Bianchini, C.; Mealli, C.; Meli, A.; Orlandini, A.; Sacconi, L. *Inorg. Chem.* **1980**, *19*, 2968. (b) Dapporto, P.; Midollini, S.; Orlandini, A.; Sacconi, L. *Ibid.* **1976**, *15*, 2768. (c) Bianchini, C.; Masi, D.; Mealli, C.; Meli, A. *J. Organomet. Chem.* **1983**, *247*, C29. (d) Bianchini, C.; Meli, A.; Scapacci, G. *Organometallics* **1983**, *2*, 1834.
(4) Mealli, C.; Hoffmann, R.; Stockis, A. *Inorg. Chem.* **1984**, *23*, 56.

0020-1669/84/1323-2838$01.50/0

Table I. Crystal Data and Experimental Variables for X-ray Diffraction

	(triphos)Ni(η^2-CS_2) (**2**)	(triphos)Ni(η^2-SCNPh)·0.5CH_2Cl_2 (**3**)	(np_3)Co(η^2-SCNPh)·1.33C_4H_9OH (**4**)
molecular formula	$C_{42}H_{39}NiP_3S_2$	$C_{48.5}H_{45}ClNNiP_3S$	$C_{54.33}H_{60.33}CoNO_{1.33}P_3S$
mol wt	759.54	861.05	932.44
cryst syst	orthorhombic	orthorhombic	monoclinic
space group	$Pn2_1a$	$Pbac$	$P2_1/a$
a, Å	20.924 (9)	23.142 (7)	36.435 (11)
b, Å	17.112 (8)	21.429 (7)	10.801 (7)
c, Å	10.283 (5)	17.204 (6)	13.026 (8)
β, deg			97.62 (9)
V, Å^3	3681.84	8531.62	5080.91
Z	4	8	4
ρ(calcd), g cm^{-3}	1.37	1.34	1.21
ρ(measd), g cm^{-3}	1.36	1.33	1.19
μ, cm^{-1}	7.54	7.10	5.03
color	dark brown	red	brick red
habit	parallelepiped	parallelepiped	parallelepiped
dimens, mm	0.16 × 0.16 × 0.26	0.36 × 0.15 × 0.12	0.40 × 0.11 × 0.10
no. of reflcns measd	6340 [hkl]	7740 [hkl]	7361 [$\pm h,+k,+l$]
no. of reflcns with [$I > 3\sigma(I)$]	2104	1499	2123
scan type	ω-2θ	ω-2θ	ω-2θ
$2\theta_{max}$, deg	40	50	45
radiation	Mo Kα	Mo Kα	Mo Kα
wavelength, Å	0.7107	0.7107	0.7107
scan range, deg	1	0.9	0.9
scan speed, deg/s	0.06	0.05	0.05
cryst decay	no decay	no decay	no decay
R^a	0.048	0.072	0.074
$R_w{}^b$	0.0471	0.078	0.078

[a] $R = \Sigma||F_o| - |F_c||/\Sigma|F_o|$. [b] $R_w = [\Sigma w(|F_o| - |F_c|)^2/\Sigma w|F_o|^2]^{1/2}$.

Solution and Refinement of the Structures. The initial nonhydrogen atom coordinates of **2** were those previously reported for the isomorphous compound **1**.[3a] The other structures were solved by Patterson and Fourier methods. The SHELX76 system[5] was used for all the crystallographic computing. The positional and thermal parameters were refined by using the full-matrix least-squares technique. The minimized function was $\sum w(|F_o| - |F_c|)^2$ where $w = 1/\sigma^2(F_o)$. The phenyl groups were treated as rigid bodies with D_{6h} symmetry (C–C = 1.39 Å). The H atoms were located in their idealized positions (C–H = 0.95 Å). The structures of **3** and **4** show the presence of solvent molecules: dichloromethane and butanol, respectively. The former molecule is on a crystallographic twofold axis. Some disorder problem is connected with the presence of butanol in **4**. Two different regions of the cell are occupied by butanol. The refined population parameter for each molecule is 0.69 and 0.64, respectively, for a total of 1.33 butanol molecules for each complex unit: this result is in nice agreement with the elemental analysis. The final R factors for structures **2**–**4** are reported in Table I. An appropriate test based on the anomalous scattering confirms that the chirality of **2** is the same as that of the isomorphous complex **1**.[3a] In fact, a refinement based on a structure with $x,\bar{y},z$ coordinates gave an R value 0.04 higher than that given by the structure x,y,z. Final difference syntheses with residual peak heights less than 0.7 e/Å^3 for all of the compounds showed no anomalous features. Atomic scattering factors and correction for anomalous dispersion effects were determined by using the coefficients reported in ref 6. Tables of observed and calculated structure factors are available as supplementary material. Tables II–IV contain the coordinates for nonconstrained atoms as obtained by the final least-squares cycles. Tables deposited as supplementary material contain coordinates for rigid-group atoms and hydrogen atoms and temperature factor for the atoms of Tables II–IV.

Results and Discussion

Comparison between the Structures. The complexes **1**–**4** all present a constant primary geometry where a metal fragment of L_3M type, formed by the metal and three phosphorus atoms of the tripodal ligand (triphos or np_3), is η^2 bonded to a C–S linkage of the heteroallene (CS_2 or SCNPh). Notice that, although the ligand np_3 contains a fourth donor atom (nitrogen) beside three phosphorus atoms, this is far away from the metal in **4** (3.44 (1) Å) so that the metal fragment can be also described of the L_3M type. Figures 1–4 show views of the skeleton of the complexes perpendicular to the plane defined by the metal, carbon, and sulfur atoms (side a) and down the trace of the threefold axis of L_3M (side b). Selected bond distances and angles for compounds **1**–**4** are reported in Table V.

Table II. Atomic Coordinates for (triphos)Ni(η^2-CS_2) (**2**)

atom	x	y	z
Ni	−654 (1)	−1321	691 (1)
P(1)	376 (1)	−1273 (2)	1274 (3)
P(2)	−541 (1)	−121 (2)	−275 (4)
P(3)	−974 (1)	−838 (2)	2595 (3)
S(1)	−807 (2)	−2453 (2)	−264 (5)
S(2)	−2143 (2)	−1825 (3)	−26 (5)
C	−1378 (5)	−1844 (6)	110 (11)
C(1)	360 (5)	971 (6)	2874 (10)
C(2)	60 (4)	252 (5)	2196 (8)
C(3)	614 (4)	−270 (5)	1740 (9)
C(4)	−342 (4)	574 (5)	1066 (8)
C(5)	−346 (4)	−184 (5)	3224 (8)

Table III. Atomic Coordinates for (triphos)Ni(η^2-SCNPh)·0.5CH_2Cl_2 (**3**)

atom	x	y	z
Ni	7417 (1)	1639 (1)	3344 (2)
P(1)	8223 (3)	1896 (3)	3960 (4)
P(2)	7684 (3)	626 (3)	3342 (4)
P(3)	6907 (3)	1684 (3)	4392 (4)
S(1)	7356 (3)	2150 (3)	2197 (4)
N(1)	6279 (9)	1646 (10)	2563 (11)
C	6809 (11)	1774 (12)	2641 (14)
C(1)	8024 (10)	567 (11)	5751 (11)
C(2)	7842 (9)	897 (11)	4995 (12)
C(3)	8336 (10)	1366 (11)	4809 (12)
C(4)	7768 (11)	378 (11)	4368 (12)
C(5)	7271 (9)	1240 (10)	5182 (11)
C(7)	0	−403 (26)	5000
Cl(1)	490 (5)	243 (5)	4637 (6)

(5) Sheldrick, G. M. "System of Computing Programs"; University of Cambridge: Cambridge, England, 1976.
(6) "International Tables for X-ray Crystallography"; Kynoch Press: Birmingham, England, 1974; Vol. IV, p 99.

Table IV. Atomic Coordinates for $(np_3)Co(\eta^2\text{-}SCNPh)\cdot 1.33C_4H_9OH$ (4)[a]

atom	x	y	z
Co(1)	3727 (1)	7482 (2)	−805 (2)
P(1)	3998 (1)	7180 (4)	877 (3)
P(2)	3224 (1)	8647 (4)	−545 (3)
P(3)	3485 (1)	5574 (4)	−1171 (4)
S(1)	4179 (1)	8478 (5)	−1444 (4)
N(1)	3179 (3)	6358 (11)	941 (9)
N(2)	3588 (4)	8119 (12)	−3051 (11)
C(1)	3722 (4)	7228 (14)	1956 (12)
C(2)	3416 (4)	6253 (15)	1901 (13)
C(3)	3060 (4)	5195 (13)	461 (12)
C(4)	2814 (4)	7926 (15)	−117 (12)
C(5)	3356 (4)	4622 (13)	−104 (11)
C(6)	2883 (4)	7269 (14)	920 (12)
C(7)	3763 (4)	8057 (14)	−2145 (12)
O(1)*	3709 (8)	3736 (29)	4174 (22)
C(8)*	3350 (12)	3110 (43)	4524 (35)
C(9)*	3308 (12)	4006 (42)	5346 (35)
C(10)*	3467 (13)	5265 (44)	4978 (35)
C(11)*	3728 (13)	4927 (45)	4347 (36)
O(2)*	−44 (9)	2826 (28)	4333 (25)
C(12)*	−131 (13)	2389 (44)	5201 (39)
C(13)*	176 (14)	1841 (44)	5836 (39)
C(14)*	486 (13)	2000 (44)	5137 (40)
C(15)*	326 (14)	2442 (44)	4177 (38)

[a] Atoms marked with an asterisk belong to the solvent molecules.

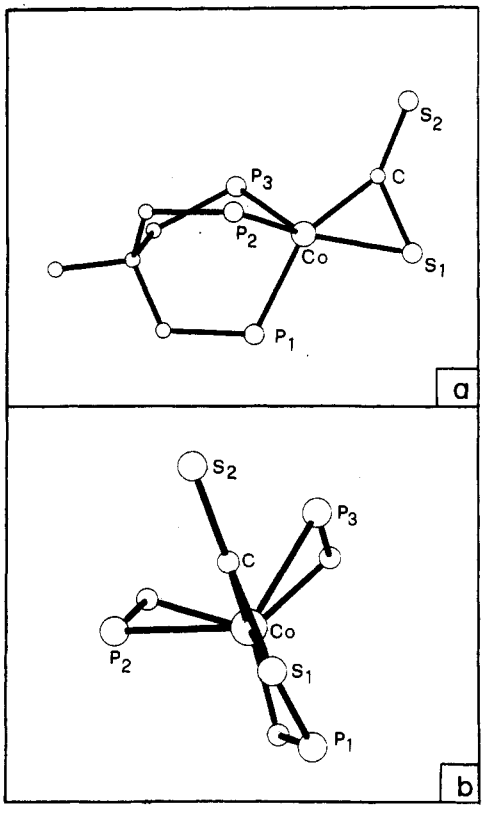

Figure 1. (a) Side view of the skeleton of (triphos)Co(η^2-CS_2). (b) Top view of the same skeleton.

The most straightforward comparison is done between compounds **1** and **2**. Chemically they differ only for the nature of the metal: a d^9 cobalt(0) in **1** and d^{10} nickel(0) in **2**. Accordingly, the compounds are paramagnetic for one unpaired electron (**1**) or diamagnetic (**2**). By examining their structures, one could hardly detect any major geometrical difference between the complexes that are indeed structurally isomorphous. As seen in Figures 1 and 2 one of the phosphorus atoms, P(1), is contained in the plane of CS_2, which also is the mirror plane for the skeleton of the complexes. The values

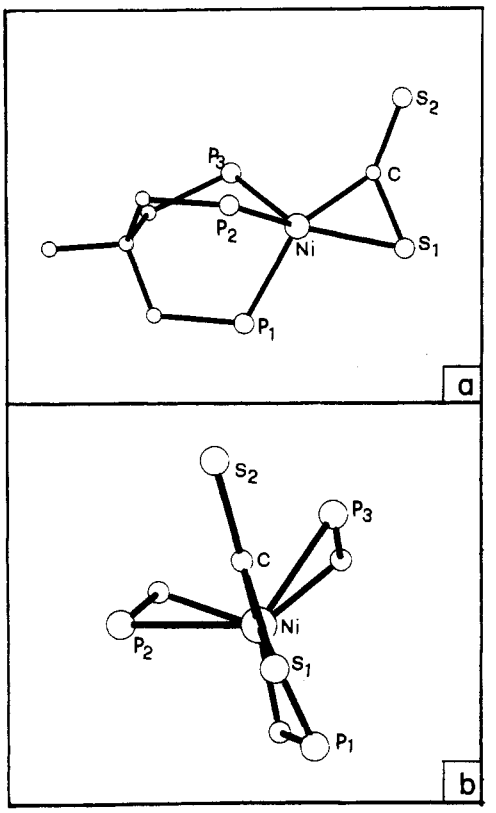

Figure 2. (a) Side view of the skeleton of (triphos)Ni(η^2-CS_2). (b) Top view of the same skeleton.

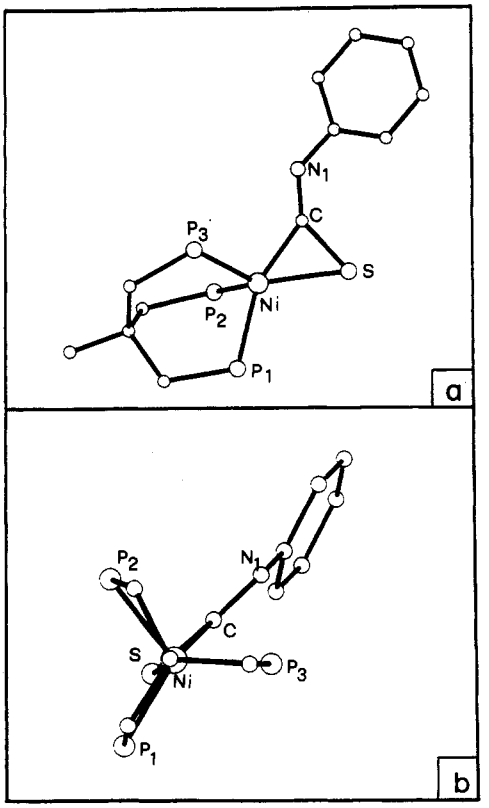

Figure 3. (a) Side view of the skeleton of (triphos)Ni(η^2-SCNPh). (b) Top view of the same skeleton.

of the P–M–P angles are all very close to 90° (largest deviation from this value is 2.3° in **1** and 4.7° in **2** and are consistent with an hemioctahedral geometry of the L_3M fragment. The M–P distances average 2.23 (1) Å in **1** and 2.26 (3) Å in **2**. The geometry of the M–CS_2 fragments barely changes on

Table V. Selected Bond Distances (Å) and Angles (deg) for Structures 1-4

	(triphos)Co(η^2-CS_2)	(triphos)Ni(η^2-CS_2)	(triphos)Ni(η^2-SCNPh)	(np_3)Co(η^2-SCNPh)
M-P(1)	2.247 (3)	2.240 (2)	2.215 (6)	2.303 (4)
M-P(2)	2.232 (3)	2.296 (3)	2.258 (6)	2.286 (4)
M-P(3)	2.222 (3)	2.235 (2)	2.156 (6)	2.269 (4)
M-S(1)	2.206 (4)	2.197 (3)	2.259 (6)	2.220 (5)
M-C	1.88 (1)	1.86 (1)	1.88 (2)	1.87 (2)
C-S(1)	1.68 (1)	1.63 (1)	1.68 (2)	1.72 (2)
C-X[a]	1.62 (1)	1.61 (1)	1.26 (2)	1.27 (2)
P(1)-M-P(2)	89.2 (1)	89.2 (1)	90.6 (2)	100.8 (2)
P(1)-M-P(3)	91.9 (1)	92.2 (1)	92.8 (2)	100.2 (2)
P(2)-M-P(3)	92.3 (1)	94.7 (1)	101.2 (2)	103.5 (2)
P(1)-M-S(1)	106.2 (1)	107.0 (1)	110.5 (3)	100.4 (2)
P(2)-M-S(1)	130.7 (1)	127.5 (1)	118.8 (2)	116.0 (2)
P(3)-M-S(1)	132.2 (1)	132.6 (1)	132.4 (3)	130.5 (2)
C-M-S(1)	47.7 (4)	46.5 (3)	46.9 (7)	48.9 (4)
S(1)-C-X	133.8 (8)	136.1 (7)	141.8 (2.0)	141.1 (1.3)
M-C-S(1)	76.3 (5)	77.7 (4)	78.5 (1.0)	76.0 (7)
M-S(1)-C	57.4 (5)	55.7 (4)	54.5 (8)	55.0 (5)
M-C-X	149.9 (8)	146.1 (7)	139.6 (2.0)	142.8 (1.2)
P(1)-M-C	153.3 (4)	152.7 (3)	154.3 (8)	149.2 (6)
P(2)-M-C	112.1 (4)	112.0 (3)	110.6 (7)	96.4 (6)
P(3)-M-C	102.7 (4)	102.6 (3)	96.9 (7)	100.3 (6)

[a] X = S in **1** and **2**, X = N in **3** and **4**.

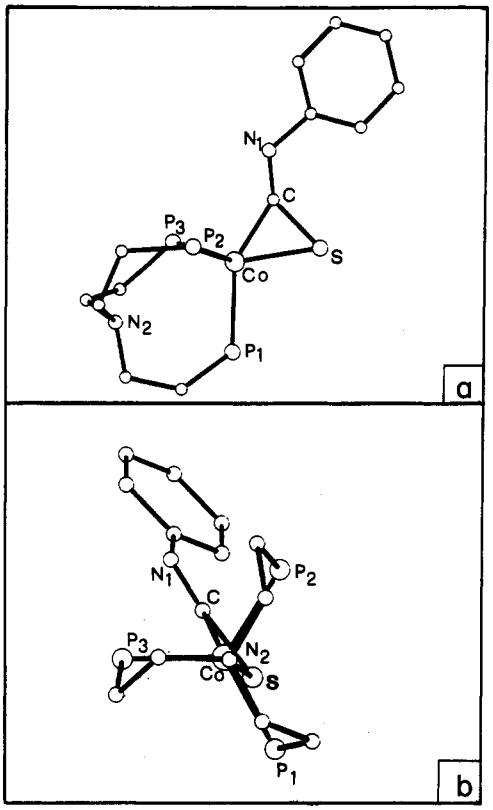

Figure 4. (a) Side view of the skeleton of $(np)_3Co(\eta^2$-SCNPh). (b) Top view of the same skeleton.

going from **1** to **2**: the coordinated C–S linkage is slightly longer in the cobalt derivative (1.68 (1) vs. 1.63 (1) Å) whereas the amount of bending of the CS_2 molecule is somewhat more pronounced in the same complex (S–C–S = 133.8 (8) vs. 136.1 (7)° in **1** and **2**, respectively). It is however hard to establish any systematic differential trend attributable to the different nature of the metals. The fact that both the M–C and M–S distances are almost perfectly matched (see Table V) in **1** and **2** does not allow in principle the conclusion that the Co–C interaction is as strong as the Ni–C interaction or that the energetics of the Co–S and Ni–S bonds are comparable.

Next, we compare the geometries of compounds **2** and **3**. Here, the same (triphos)Ni fragment is interacted with two heteroallenic molecules that differ in the nature of the terminal groups, namely a sulfur atom in **2** and a NPh grouping in **3**. Some evident rearrangements have occurred in the geometry of the $P_3Ni(\eta^2$-CS) fragment in the structure of **3**. Very interestingly there is an unexpected descent of the symmetry of the P_3Ni fragment from C_{3v} to C_s; in fact, one of the P–Ni–P right angles, P(2)–Ni–P(3), opens up to 101.2 (2)°. Moreover, the plane defined by the Ni, C, and S atoms does not contain the P(1) atom. In fact, the dihedral angle between the latter and the mirror plane of the P_3Ni fragment through P(1) is ca. 19° and the whole skeleton of the complex has only C_1 symmetry. The rearrangement of the usually rigid (triphos)M fragment[7] may be somewhat costly in terms of strain energy: what happens is readily seen by comparing Figures 2b and 3b. In **2** (and in **1** as well) the torsion angles about the C–C bond of each chain of triphos have values that deviate slightly from 170°. Conversely, in **3** two of these torsional angles are very close to 180°. In this manner triphos is allowed to open one of the P–Ni–P angles. The three M–P bonds are more asymmetrical than in **1** or **2** since their lengths vary between 2.156 (6) and 2.258 (6) Å. Quite significant for the study of the interactions between the metal fragment and the heteroallenic molecule is the lengthening of the Ni–S distance of about 0.06 Å on going from **2** to **3**; this is a clear indication of a weakened bond. At the same time, the M–C distance is almost unchanged; actually it remains constant for complexes **1**–**4** since the limiting values are 1.86 (1) and 1.88 (2) Å, respectively. It is also worthwhile to point out for subsequent considerations that the M–S vector forms with the vector defined by the two apical carbon atoms of triphos (the latter can be taken as the tripod's threefold axis) an angle of about 13°, whereas in **1**, **2**, and, in a manner, **4** as well the equivalent angle is significantly larger (between 18 and 20°).

Finally, the structure of **4** allows an evaluation of the effects induced by the simultaneous opening of the P–M–P angles up to above 100°. This is allowed by the presence of the np_3 ligand when it acts as tridentate. The P_3Co fragment maintains approximate C_{3v} symmetry. With respect to **1**, the other cobalt species under consideration, the trend is a clear lengthening of the Co–P distances (2.29 (1) Å average); conversely, a slightly longer Co–S separation (2.220 (5) vs.

(7) Many structures containing the ligand triphos acting as tridentate have been studied in this laboratory, and all show P–M–P angles that do not deviate greatly from 90°.

2.206 (4) Å) seems rather insignificant.

Other structural aspects that emerge from the comparison of the four structures are as follows: (i) A range of C–S (coordinated) bond lengths between 1.63 (1) and 1.72 (2) Å is seen. The limits are established by compounds **2** and **4**, although no clear trend emerges for these magnitudes. (ii) The bending of CS_2 is generally larger than that of SCNPh (see Table V). (iii) In any case, the coordination to the metal affects both linkages that the carbon atom forms with the adjacent atom in CS_2 and SCNPh molecules. Indeed, these linkages are shorter in the linear uncoordinated molecules [C–S = 1.55 Å in CS_2;[8] C–S = 1.578 Å, C–N = 1.205 Å in SCNR (R = *p*-bromophenyl[9])]. (iv) In compounds **3** and **4** the phenyl ring attached to the nitrogen atom is not coplanar with the SCN plane. However, there is a more pronounced torsion in **4** than in **3**, as demonstrated by the torsional angles at the N–C(Ph) bonds that are approximately 22 and 11°, respectively. Whether this difference is attributable to a sort of different electronic conjugation between the phenyl ring and the M–(η^2-SCN) fragment or more simply to different packing effects is hard to state.

MO Interpretation. With the aid of molecular orbital calculations of the extended Hückel type and the fragment orbital formalism,[10] we have attempted to interpret some of the structural trends found in compounds **1–4**. For this purpose we have used the models $(PH_3)_3M(\eta^2\text{-}CS_2)$ and $(PH_3)_3M(\eta^2\text{-}SCNH)$ (M = Co, Ni).[11] Also, the model (triphos)M(η^2-SCO) has been considered to magnify the electronegativity effects that in the SCNH model are too small to be of practical significance. Figure 5 shows an interaction diagram between the orbitals of the fragments $(PH_3)_3M$ and CS_2, which are known in detail.[12] The M–S distance is fixed at 2.20 Å whereas the angle formed by the M–S vector and the threefold axis of the L_3M fragment is 18°. The C–S and M–C distances were 1.65 and 1.87 Å, respectively. Basically the η^2 bonding in these molecules can be described by referring to the Chatt–Dewar–Duncanson model for metal–olefin complexes.[13] There are in fact two main bonding interactions. One of them corresponds to the σ-type donation from a filled π orbital of CS_2 (CS_2 1S)[14] into the empty metal sp hybrid orbital (L_3M 2S) and is shown in **1**. The other interaction,

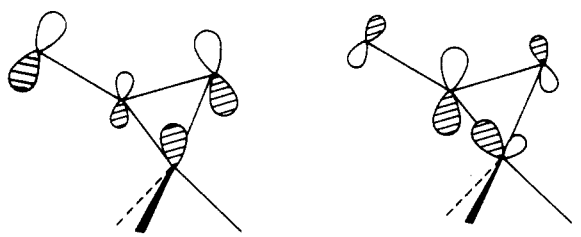

1 2

2, is the π-back-bonding donation from the symmetric metal orbital, which descends from the octahedral e_g set (the terms symmetric and antisymmetric refer to the mirror plane that coincides with the plane of the drawing) into the empty CS_2 π^* orbital (3S). Due to the relative energy gaps between the interacting orbitals the σ-type interaction is much weaker than the π-back-bonding interaction. It was also noticed how the lower combination of sulfur lone pairs (2S) mixes in the MO 1S in a destabilizing manner.[4] However, in $L_3M(\eta^2\text{-}CS_2)$ complexes, at variance with the $L_2M(\eta^2\text{-}CS_2)$ analogues,[4] the latter MO is not the HOMO: in fact, at slightly higher energy there is an antisymmetric level, largely metallic in character, that descends from the "e_g" set (1A). This level is populated by one or two electrons in **1** and **2**, respectively;[15] the different electronic population should little affect the structures, which are indeed quite similar. However, as shown in **3**, the HOMO also contains the CS_2 2A orbital (ca. 6%) in antibonding combination. Although not emphasized before,[4] this mixing is of some importance. To summarize, bonding, nonbonding, and antibonding levels are formed from the interaction of three fragment orbitals, namely those descending from the CS_2 π_u

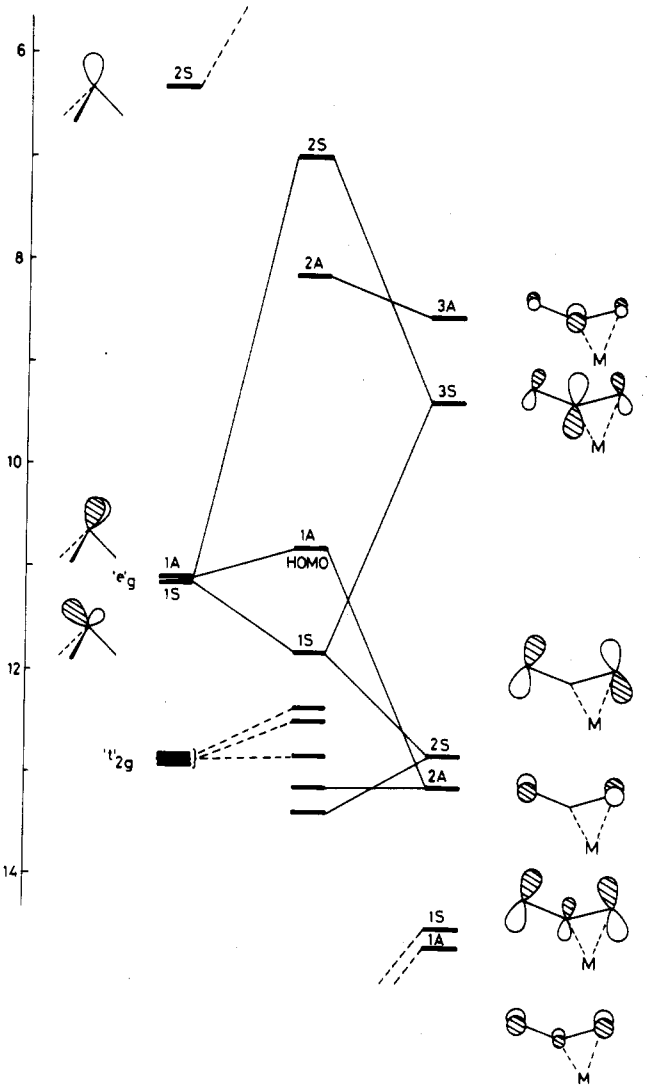

Figure 5. Interaction diagram for the model $(PH_3)_3Ni(\eta^2\text{-}CS_2)$.

(8) Guenter, A. H. *J. Chem. Phys.* **1959**, *31*, 1095.
(9) Ulicky, L. *Zb. Pr. Chemickotechnol. Fak. SVST* **1969**, *47*, 288.
(10) (a) Hoffmann, R. *J. Chem. Phys.* **1963**, *39*, 1397. (b) Hoffmann, R.; Lipscomb, W. N. *Ibid.* **1962**, *36*, 3179; **1963**, *37*, 2872. (c) Ammeter, J. H.; Bürgi, H. B.; Thibeault, J. C.; Hoffmann, R. *J. Am. Chem. Soc.* **1978**, *100*, 3686.
(11) In order to avoid a possible bias of the calculations by using a different parametrization for the metals, the cobalt atom was simulated as a Ni^+ species. Unless stated otherwise, the computational procedure, atomic parameters, and gross geometrical features are those reported in ref 4.
(12) A comprehensive description of these fragment orbitals, inclusive of the most specialized references may be found for L_3M and AB_2 fragments, respectively, in: "Molecular Structure and Bonding"; Academic Press: New York, 1979.
(13) (a) Dewar, M. J. *Bull. Soc. Chim. Fr.* **1951**, *18*, C79. (b) Chatt, J.; Duncanson, L. A. *J. Chem. Soc.* **1953**, 2939.
(14) Here, and throughout the paper, the terms symmetric (S) and antisymmetric (A) define the symmetry of the MOs with respect to the unique mirror plane of the model (usually the plane of the drawings).
(15) Experimental evidence of the correct assignment of the HOMO is provided by the powder EPR spectrum of **1**, recorded at 77 K. This is characteristic of a $S = {}^1/_2$ spin system with $g_\perp = 2.07$ and $g_\parallel = 2.17$. Accordingly the metal d orbital involved may have either xy or $x^2 - y^2$ character. If the L_3M fragment is regarded as a trigonal bipyramid where one equatorial and one axial ligand are removed (z is the main axis of the bipyramid), the metal 1A orbital is just a hybrid of those two orbitals plus some metal p character.[17]

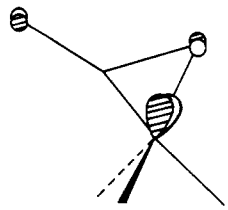

3

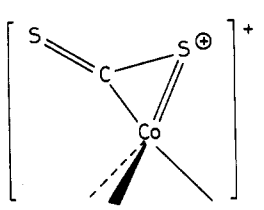

4

and π_g levels (1A and 2A) and that descending from the L_3M e_g level. On the basis of electronegativity arguments, the CS_2 orbitals involved are strongly centered on the sulfur atoms, so that the antibonding nature of the HOMO is mainly localized over the metal–sulfur linkage. The hypothetical complex $[L_3Co(\eta^2\text{-}CS_2)]^+$ would be empty at the corresponding level, hence the limiting formulation, **4**, with the M=S double bond may be acceptable. Full occupancy of the HOMO, as in **2**, cancels the M–S π bonding, whereas in **1** a residual $\pi_\perp$ interaction may still be operative. The calculations are consistent with this viewpoint: the M–S overlap drops from 0.241 to 0.168 on going from **1** to **2**. However, this idea of different bond strengths is not readily envisaged by the comparison of the Co–S and Ni–S distances found in **1** and **2**. The fact that the bonds are practically equal may just be occasional since the metallic species are different. On the other hand, we have quite good evidence that the bonding of CS_2 to the cobalt fragment is stronger than that to the nickel fragment. This evidence is based on the different chemical reactivities observed for **1** and **2**. The arguments will be summarized in a forthcoming paper,[16] but generally we observe an easy rupture of the Ni–CS_2 linkage upon attack of several chemical reagents, whereas the cobalt species is much more resistant.

The next step is to look at the electronic effects for replacing the uncoordinated sulfur atom with a more electronegative atom or grouping, in light of a structural comparison between **2** and **3**. In the latter complex there is an opening of one P–Ni–P angle, a rotation of the plane defined by Ni, C, and S atoms that destroys the C_s symmetry of the molecule, and finally a significant lengthening of the Ni–S distance. With respect to the diagram of Figure 5, the presence of a more electronegative atom in the heteroallenic fragment produces a lowering in energy of the frontier orbitals, which however maintains the relative ordering. There is also a different composition of these orbitals in terms of atomic orbitals. Thus, the orbitals 2A and 2S, considered in CS_2 equally weighted combinations of the sulfur lone pairs, in SCO become heavily centered of the sulfur atom, as shown in **5** and **6** by the relative

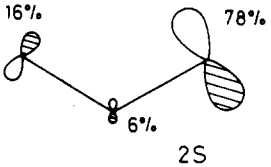

5

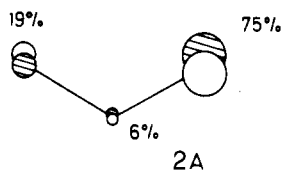

6

percentages of the single atomic orbitals. Conversely, orbitals 3S and 3A are not greatly affected in this respect. The proper evaluation of these effects over the construction of the interaction diagram with the orbitals of the L_3M fragment is not immediate. Although the model considered has still the highest possible symmetry, C_s (with local C_{3v} symmetry for the L_3M fragment), the asymmetry of COS further complicates the orbital mixing. Thus, on going from CS_2 to SCNH to SCO we observe a progressive reduction of the 2S (heteroallenic) orbital in the MO 1S, which is the main bonding orbital between the two fragments. As was previously pointed out,[4] it is this destabilizing mixing that prevents too large of a bending of the CS_2 molecule in the complex. At variance, CO_2 is predicted by extended Hückel methods to have unrealistically small O–C–O angles just because no O–O antibonding orbital equivalent of 2S is at a sufficiently high energy to mix into MO 1S; the behavior of SCNH and SCO molecules is intuitively intermediate in this respect. Also, the other important bonding interaction between the metal 2S and heteroallene 1S orbitals changes in character. Due to the progressively larger gap between those two orbitals, the higher heteroallene 2S combination overtakes the role of 1S as a donor toward the metal. This orbital is heavily centered on sulfur as shown in **6**. Accordingly, the hypothetical η^2-coordinated C–S bond of SCO would donate to the metal mainly through a sulfur lone pair rather than through a S–C π bond, and the essence of the Chatt–Dewar–Duncanson model would be consequently modified. Significantly the sulfur atom in **3** is more vertically displaced over the P_3Ni fragment. The structure of **3** also shows another significant distortion: the opening of one P–Ni–P angle. This fact was also ascertained with other polyphosphinic tripodal ligands and studied in terms of MO theory[17] but is unprecedented for the rigid (triphos)M fragments. The e_g orbitals (1S and 1A in Figure 5) are most affected by the distortion, and their degeneracy is removed. Whereas 1A drops energy becoming less hybridized, the symmetric partner 1S is slightly destabilized and its largest lobe reoriented as to lie more collinear with the trans Ni–P vector. Also, the total energy of the fragment is lowered and generally a stabilization of the complex ensues. However, in the case of triphos the energetic benefit is probably nullified by the strain induced at the ethylenic chains. The lowering of the metal 1A orbital accompanies a reduced energy gap with the heteroallenic 2A orbital so that their reciprocal four-electron destabilizing interaction becomes more pronounced. Also, the overlap argument works to make this destabilization larger in **3** than in **2** both because the orbital 2A (**6**) is more developed at the sulfur atom and because the sulfur atom is more vertical over the L_3Ni fragment. The lengthening of the Ni–S distance in **3** vs. **2** is very likely attributable to these effects. It cannot be excluded that the reorientation of the plane defined by Ni, S, and C atoms with respect to the L_3M fragment, as observed in **3**, serves to reduce the above destabilizing effects, but the computed energy surface for this rearrangement is very soft. Indeed, L_3MCX_2 complexes, at variance with L_2MCX_2 species, were previously predicted to have no appreciable barrier for the rotation of the coordinated C–X bond around the symmetry axis of the metal fragment.[4]

In summary, on account of the different electronegativity of the uncoordinated group, the composition of the frontier orbitals of heteroallene is changed. Thus, the slipping of the C–S linkage with respect to the metal fragment favors the σ bonding by taking advantage of the localization of the 2s orbital on sulfur. On the other hand it triggers $\pi_\perp$ repulsive interactions. The electronegativity perturbation in SCO is far larger than that in SCNPh, and it may well be that a drastic rearrangement of the metal fragment is necessary to stabilize η^2-coordinated SCO complexes. The (triphos)M fragment hardly tolerates a distortion more pronounced than that in **3**, and ultimately here we find a hint to account for the known instability of $M(\eta^2\text{-SCO})$ complexes.

In complex **4** the geometry seems to be less strained than in **3**. The L_3M fragment maintains approximate C_{3v} symmetry, but the P–Co–P angles are opened up to above 100°, a fact easily allowed by the more flexible chains of np_3. Such a loss of pyramidalization lowers the energy of the P_3Co

(16) Bianchini, C.; Mealli, C.; Meli, A., manuscript in preparation.

(17) Mealli, C.; Midollini, S.; Moneti, S.; Albright, T. A. *Helv. Chim. Acta* **1983**, *66*, 557.

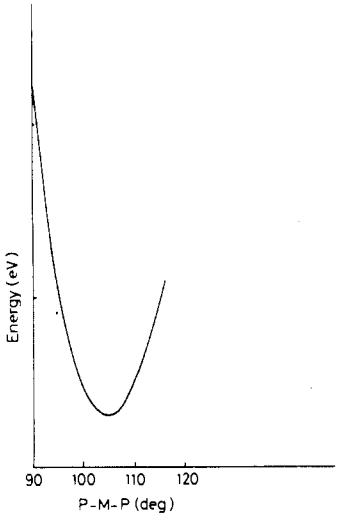

Figure 6. Total energy variation for the model $(PH_3)_3Co(\eta^2\text{-SCNH})$ on opening the three P–Co–P angles from 90°.

fragment and that of the whole complex as shown by the plotting of the total energy of the $(PH_3)_3Co(\eta^2\text{-SCNPh})$ model as a function of the P–Co–P angles in Figure 6. A minimum is calculated at angles of approximately 103° not too far from the experimental values. It was previously pointed out for $L_3Ni(\eta^3\text{-cyclopropenium})$ complexes,[17] and holds for the present complexes as well, that the gain of the total energy corresponds to a weakening of the linkage between the interacting fragments. Here, there is about a 20% decrease of the overlap between P_3Co and SCNH fragments on opening the P–Co–P angles from 90 to 104°. One of the reasons for this is that the e_g orbitals of Figure 5, while are both lowered in energy, become less hybridized and in general overlap less with the heteroallenic orbitals. Also the energy gap argument predicts a lower interaction of type **2**. Perhaps significantly the Co–S distance is slightly longer in **4** than in **1** on account of the same $\pi_\perp^*$ argument that justified the difference between the Ni–S distances in **3** and in **2**. However, in the presence of d^9 metals the $\pi_\perp^*$ orbital is only half-populated and the effect less marked.

Conclusions and Extensions. The comparative study of complexes **1**–**4** has clarified some aspects of the bonding of heteroallenes toward d^9 or d^{10} L_3M fragments. The structural details confirm the computational results that the HOMO is a metal-centered orbital having $\pi_\perp$ character with a some mixing in antibonding fashion, of a $\pi_\perp$ orbital of CS_2 centered at the sulfur atoms. The LUMO (MO 2A, see Figure 5) is also a $\pi_\perp$ orbital centered on the CS_2 molecule and has C–S antibonding character; moreover, this orbital is largely developed at the carbon atom.

The knowledge of the frontier orbitals is very important in interpreting the chemical reactivity of complexed heteroallenes.

The often invoked similarity[18] between carbene and η^2-heteroallene mononuclear complexes, with respect to nucleophilic attack, may depend on the fact that both types of complexes have LUMOs centered at the α-carbon atom.[19] In the case of CS_2 complexes a nucleophilic attack may sometime lead to the rupture of a C–S bond due to the CS_2 $\pi_\perp^*$ nature of the LUMO.[20] Electrophilic attack usually takes place to β atoms in both species, and we know that the MO 1S (Figure 5) is largely a lone pair developed at the uncoordinated sulfur.[4]

Finally, we note the radical nature of compound **1**: one electron in a largely metallic orbital. It is reasonable that its chemical reactivity, which is in many respect unique, is of the radical type. In this context the reactions of **1** toward O_2, S_8, and Se[21] can be viewed as following a pathway where the requirement is the splitting of these reactants into radicals.

The study of the specific chemical reactivity, of the $L_3M(\eta^2\text{-}CS_2)$ complexes mainly developed in this laboratory, is under way.

Registry No. **1**, 74244-56-7; **2**, 60294-99-7; **3**, 86567-91-1; **4**, 87306-35-2.

Supplementary Material Available: Listings of structural parameters for the atoms of the phenyl rings refined as rigid bodies, coordinates of H atoms, thermal parameters for the refined atoms, and observed and calculated structure factor amplitudes (42 pages). Ordering information is given on any current masthead page.

(18) (a) Le Bozec, H.; Dixneuf, P. H.; Carty, A. J.; Taylor, N. J. *Inorg. Chem.* **1978**, *17*, 2568. (b) Fachinetti, G.; Floriani, C.; Chiesi-Villa, A.; Guastini, C. *J. Chem. Soc., Dalton Trans.* **1979**, 1612.
(19) (a) Kostic, N. M.; Fenske, R. F. *J. Am. Chem. Soc.* **1982**, *104*, 3879. Kostic, N. M.; Fenske, R. F. *Organometallics* **1982**, *1*, 974.
(20) Werner, H. *Coord. Chem. Rev.* **1982**, *43*, 175 and references therein.
(21) Bianchini, C.; Meli, A. *J. Chem. Soc., Chem. Commun.* **1983**, 156.

Contribution from the Division of Earth and Physical Sciences, The University of Texas at San Antonio, San Antonio, Texas 78285

Octahedral–Tetrahedral Geometry Changes for Zinc(II) in the Presence of Chloride Ions

HERBERT B. SILBER,* DEXTER SIMON, and FERENC GAIZER[1]

Received October 12, 1983

Ultrasonic absorption measurements have been carried out at 25 °C on 0.400 M zinc chloride solutions in aqueous DMF and methanol. An octahedral to tetrahedral geometry change occurs above a water mole fraction of 0.5 in both systems, and the solvation shell consists of water in both solvent systems. A similar change had been previously observed in aqueous Me_2SO. In aqueous methanol even at low water mole fractions where the solvation shell consists of both water and methanol, this geometry change is detected in the presence of any water.

Introduction

Zinc ions have been known to be important in biological systems for approximately 100 years, but only over the last 30 years have zinc-containing systems been increasingly studied.[2] Because zinc(II) is transparent to normal optical spectroscopic radiation, information about the mechanism and geometry at the metal site is normally obtained by indirect techniques such as kinetics or by substitution of the zinc by

(1) On leave from the College of Food Technology, Department of Chemistry, Hodmezovasarhely, Hungary, 1979.

(2) Prasad, A. S. In "Metal Ions in Biological Systems"; Sigel, H., Ed.; Marcel Dekker: New York, 1982; Vol. 14, pp 37–55.

0020-1669/84/1323-2844$01.50/0